Article

Growth of Calcite in Confinement

Lei Li [1], Felix Kohler [2], Anja Røyne [3] and Dag Kristian Dysthe *

University of Oslo, Department of Physics, Condensed matter section and Physics of Geological Processes, POBox 1048 Blindern, 0316 Oslo, Norway

[1] lei.li@fys.uio.no

[2] felix.kohler@fys.uio.no

[3] anja.royne@fys.uio.no

* Correspondence: d.k.dysthe@fys.uio.no; Tel.: +47-90940996

Abstract: Slow growth of calcite in confinement is abundant in Nature and man made materials. There is ample evidence that such confined growth may create forces that fracture solids. The thermodynamic limits are well known but since confined crystal growth is transport limited and difficult to control in experiment we have almost no information on the mechanisms or limits of these processes. We present a novel approach to in situ study of confined crystal growth using microfluidics for accurate control of the saturation state of the fluid and interferometric measurement of the topography of the growing confined crystal surface. We observe and explain the diffusion limited confined growth structures observed and can measure the crystal "floating" on a fluid film of 10-40 nm thickness due to the disjoining pressure. We find that there are two end member behaviours: smooth or intermittent growth in the contact region, the latter being faster than the former.

Keywords: crystal growth; calcite; microfluidic; nanoconfinement; reflection interference contrast microscopy.

1. Introduction

A number of marine organisms mineralize calcium carbonate[1]. The biomineralization processes are of great interest in themselves and confinement in cellular compartments is thought to be important in the process of controlling biological mineral growth[2]. The organisms with calcium carbonate skeletons sediment and the sediments undergo compaction where dissolution and recrystallization of calcite occurs in confinement to form limestone [3]. Some such carbonate rocks are buried deeper and undergo recrystallization in confinement once more and emerge as marble. Both limestone and marble are used for construction and sculptures that deteriorate due to confined salt crystallization in the pore space [4]. Calcite is also used in many industrial processes from paper whitening and pharmaceutical pills to cement production. In Portland cement CO_2 is slowly adsorbed and calcite is crystallized in confinement [5]. Confined recrystallization of calcite in other environments has also been shown to create forces that break other mineral grains [6] and lift rock overburden [7].

Crystal growth from solution in a spatially confined environment is in general limited by diffusion of their constituents through the solution to the growing surface. If there is some force pressing the growing crystal against an impermeable solid there may still be a confined fluid film between the two solid surfaces supporting the load [8,9]. Straightforward reasoning suggests that there will be a negative feedback between growth and transport in the confined fluid. If the fluid supports sufficient stress one expects a well defined growth rim to appear at the confined growing surface [10]. Earlier studies of crystal growth confined by a glass plate and creating a force have been performed on ionic crystals like potassium alum [11] and $NaClO_3$ [12]. These experiments show, however that the confined growth surface is much more complex which signifies that there are other, positive feedback mechanisms at work. The experiments are not in accord with existing continuum theories of confined crystal growth and force of crystallization [12].

Here we report confined crystal growth experiments that differ from previous experiments in two respects: 1) In stead of highly soluble ionic crystals we use calcite which has a solubility about 4

orders of magnitude smaller and the growth constant is 3-4 orders smaller than $NaClO_3$. 2) We study the evolution of the growing confined crystal surface in situ. By using reflected interference contrast microscopy (RICM) we may measure the distance from the confining surface to the crystal surface while it evolves.

2. Results

We will present many images of how the crystal surfaces confined by the glass surface evolve. We will quantify and summarize the common behaviour and display the variations in growth habit that may help us and the reader to interpret the reasons for the variability in quantifiable parameters.

2.1. Interpretation and quantification of in situ image data

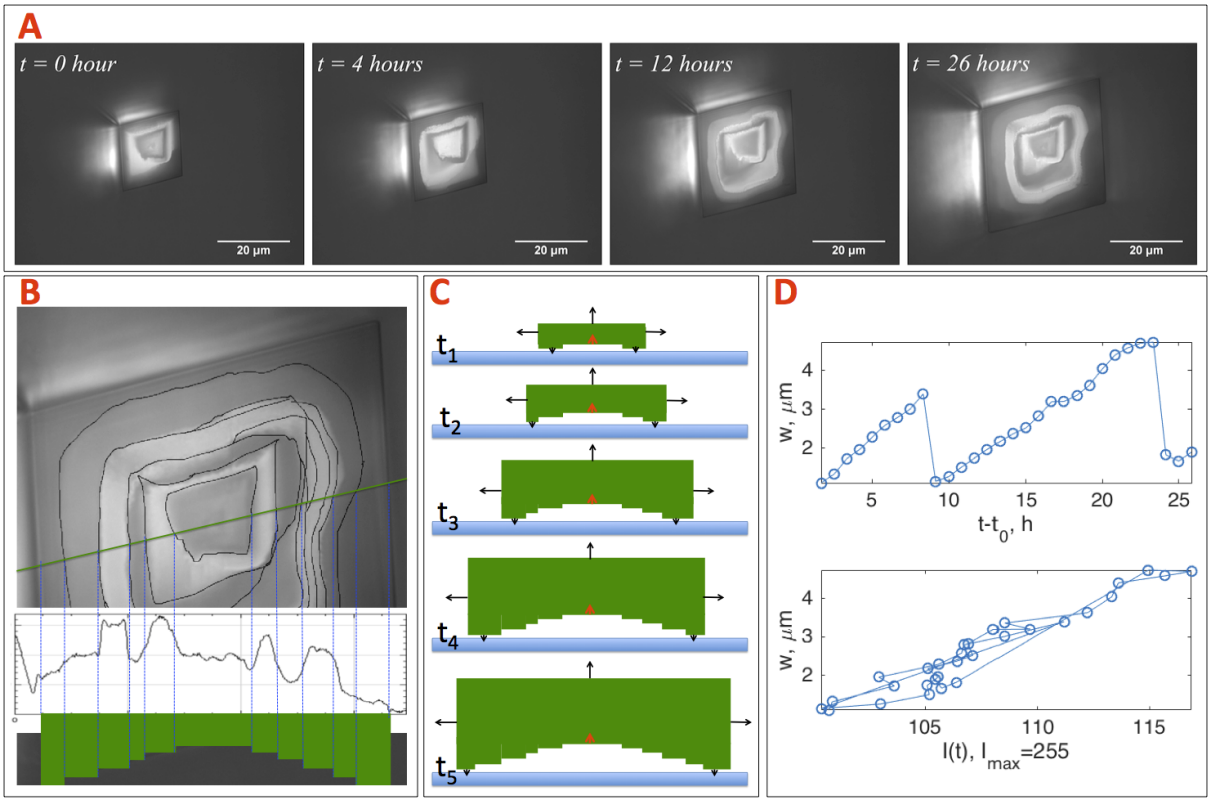

Figure 1. 26 hours growth of crystal A, primary data and interpretations. The Ca^{2+} concentration here was 0.8 mM and flow direction from bottom to top in images. **A:** In situ images of growing 104 calcite crystal surface confined by glass, imaged from below (See Materials and methods and Figure 9). For full timelapse movie of the same crystal, see movie S1.avi. Dark areas along the rim of the crystal signify areas of contact between crystal and glass. **B, Top:** Lines of inner rim edge position of crystal A at different times is drawn on the final crystal surface. **B, Middle:** Intensity in image along the green line. **B, Bottom:** A sketch of a cut through the crystal along the green line showing the profile of the confined crystal surface. Vertical lines are drawn connecting the image, the intensity plot and the interpreted profile. **C:** Interpretation of the image sequence in **A**. The crystal grows outwards (black arrows) on top, outer surfaces and at the contact interface between the outer rim and the glass lifting the crystal upwards (red arrow) **D:** Rim width measured from outer edge of crystal to inner rim edge on left side of crystal along the green line versus time (top) and versus rim intensity (bottom).

Figure 1 shows the growth outwards and upwards of a crystal at $c = 0.8$ mM. Dark areas along the rim of the crystal signify areas of contact between crystal and glass. Unfortunately the imaging quality does not allow us to accurately measure the distance h_c between the crystal and the glass in the

contact region, but $h_c < 30$ nm. The change in intensity at the centre of the confined crystal surface allows us to measure the vertical growth rate of the crystal (see Materials and methods). The first 10 hours the vertical growth rate was 25 nm/h, the last 15 hours it was only 1.5 nm/h.

The area outside the crystal is much brighter on the left and upper side of the crystal than on the lower and right side due to different reflections from the different sides of the rombohedral crystal. This difference in intensity can be used to determine the orientation of the crystal.

The outwards growth rate was stable at 310±9 nm/h outwards during the entire 26 hours. It is a challenge to explain why the vertical growth rate changes even though the supersaturation and the outwards growth rate are constant. Figure 1 **C** attempts to explain how to interpret the sequence of images in **A**.

Figure 1 **B** shows crystal A after 26 hours with all the former inner boundaries of contact rims drawn in. In the video S1.avi we have drawn a line every time the outer rim contact developed a new contrast indicating that growth in the contact region stopped before reaching the former inner rim edge. One observes that the topography of steps at the confined crystal surface are relics of dynamic changes in step flow growth. The fact that they remain as steps indicates that there is very little crystal growth inside this "cavity" and that the solution inside the cavity must be at equilibrium with the crystal surface. The plot of rim width versus time at the left side of the crystal (**D:**, top plot) shows the outwards growth rate of the crystal (310±9 nm/h) and sudden jumps when the inwards confined growth of new atomic layers stops closer to the outer edge of the crystal. **D:**, lower plot shows that the intensity at the rim is directly correlated with the width of the rim. If one assumes that the lowest intensity represents full contact ($h = 0$ nm) and that maximum intensity represents $h = 100$ nm (see equation (1)) then this signifies that for this side of the crystal h is linearly dependent on the rim width and varies up and down by about 20 nm.

Assuming equal growth rate on the top and outer surfaces of the crystal the distance r from the centre of the bottom surface to the outer sides and to the top are approximately equal. The volume of the crystal is therefore approximately $V = 4r^3$. The force of the crystal resting on the contact areas of the growth rim is therefore $F = V(\rho_c - \rho_s)g$, where the crystal density is $\rho_c = 2700$ kg/m^3 and the solution density is $\rho_s = 1000$ kg/m^3. During the 26 hours shown in Figure 1 r grows linearly in time from 9 to 17 μm and the rim width w fluctuates between approximately 1 and 5 micrometers. The contact area is $A_c = 8wr$ and the pressure at the contact surface is $P = F/A_c = r^2(\rho_c - \rho_s)g/(2w)$ is in the range between 0.14 and 2.42 Pa.

2.2. *Variation in growth at nominally equal conditions*

Figure 2 shows in situ images of the confined 104 surface of crystal B with a contact rim evolution that is very distinct from crystal A. Crystal A and B may be considered representatives of two different families of behaviour that we have observed in 20-30 crystal growth experiments: smooth rim growth and intermittent rim growth, both rims actively lifting the crystal.

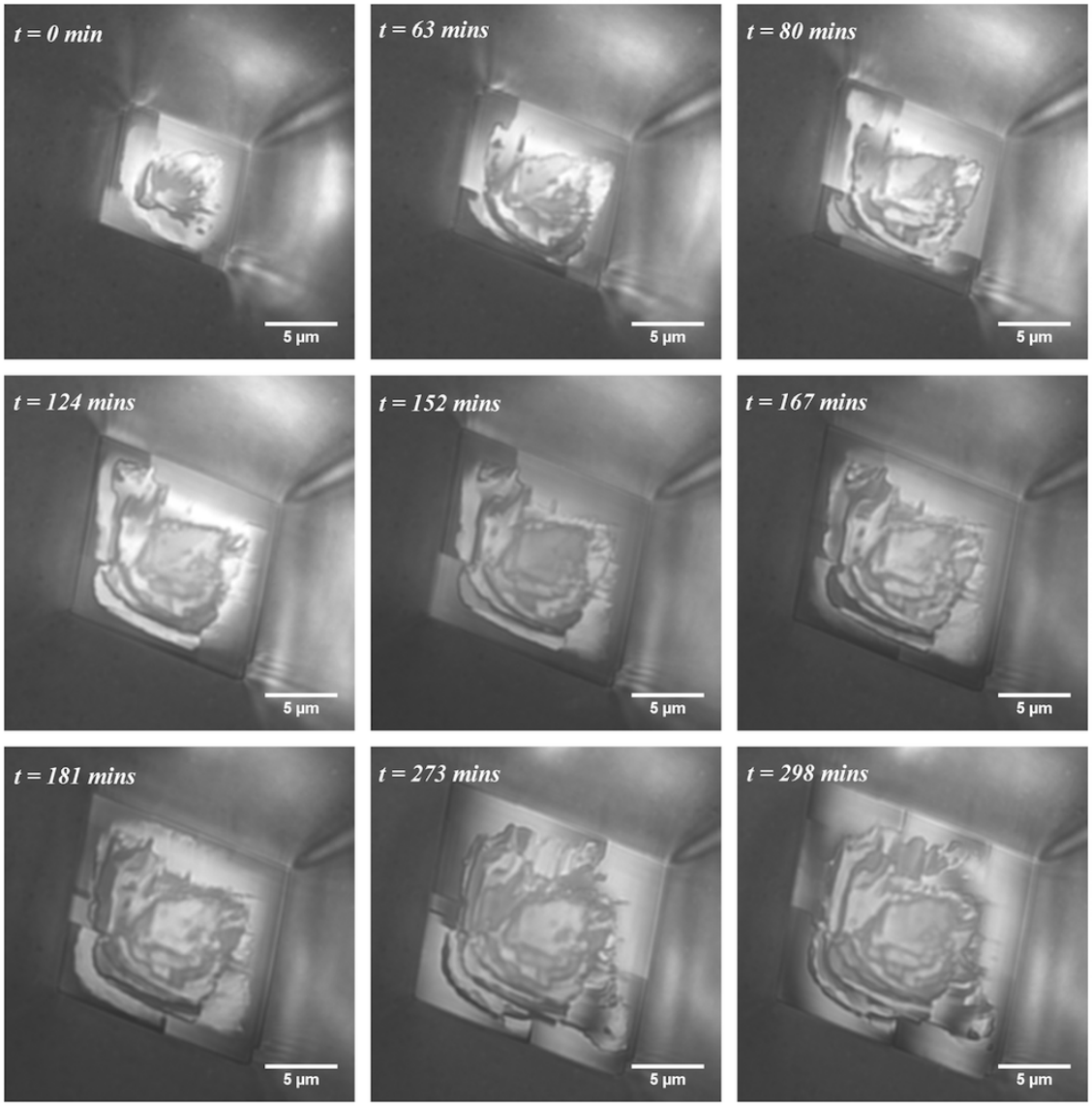

Figure 2. 6 hours growth of crystal B. The Ca^{2+} concentration here was 0.7 mM. Dark areas along the rim of the crystal signify areas of contact between crystal and glass. One observes that for crystal B these contact areas that move intermittently from place to place along the rim with time.

Crystal B grows almost 3 times faster outwards and 7 to 120 times faster upwards than crystal A even though the concentration *c* is 0.7 mM for B and 0.8 mM for A. Both crystals keep the overall rhombohedral calcite shape, but crystal B has several steps and other visible "defects" on the confined surface and on the lower right edge.

Preprints (www.preprints.org) | NOT PEER-REVIEWED | Posted: 8 August 2017 doi:10.20944/preprints201708.0028.v1

Peer-reviewed version available at Crystals 2017, 7, 361; doi:10.3390/cryst7120361

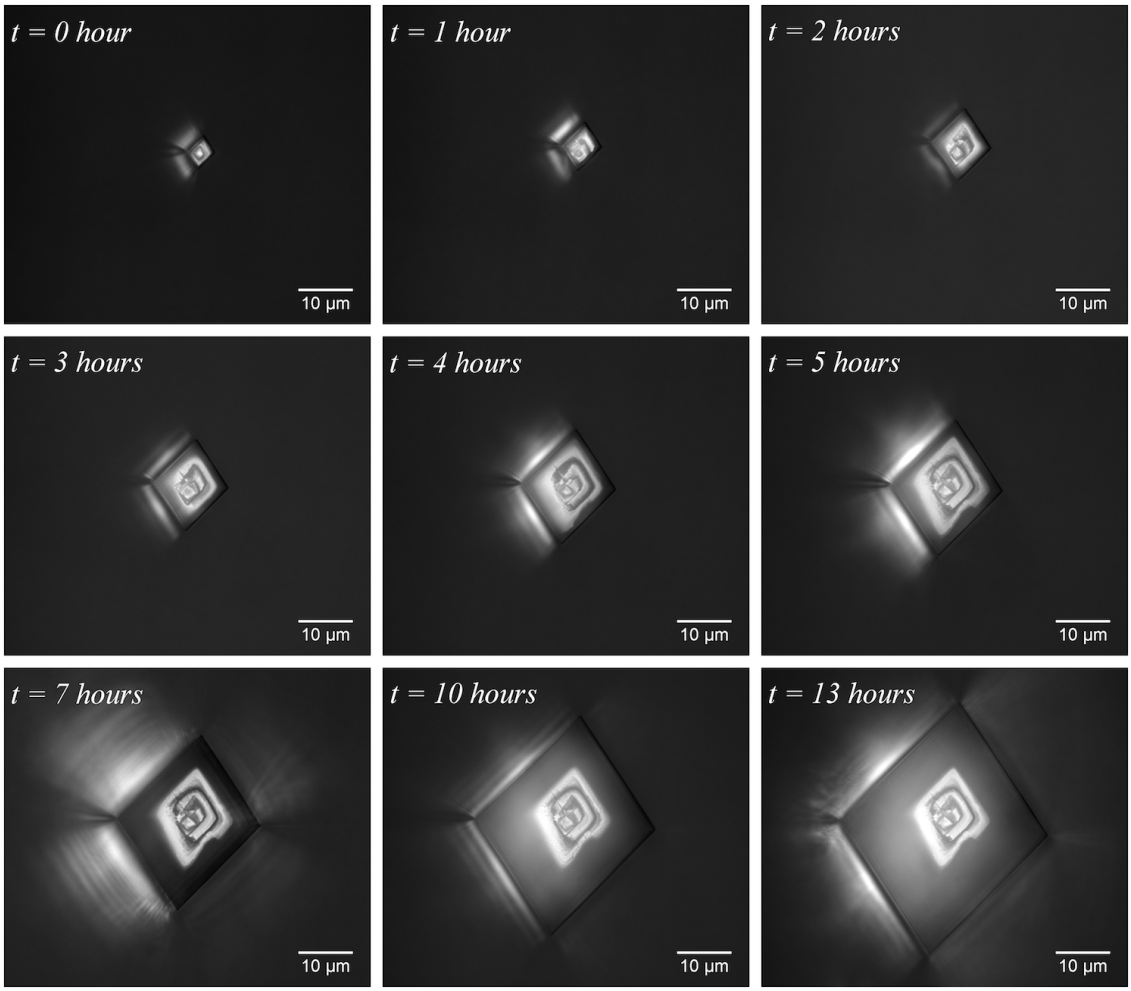

Figure 3. 13 hours growth of crystal C. The Ca^{2+} concentration here was 0.8 mM.

Crystal C in Figure 3 grows upwards at the rapid rate of 151 nm/h for the first three hours and then stops growing upwards almost completely. The inner shape and intensity of the confined surface remains constant and while the outer edge and rim width grows steadily. One may observe a very even, dark intensity around the whole contact rim signifying an even, close contact (small h).

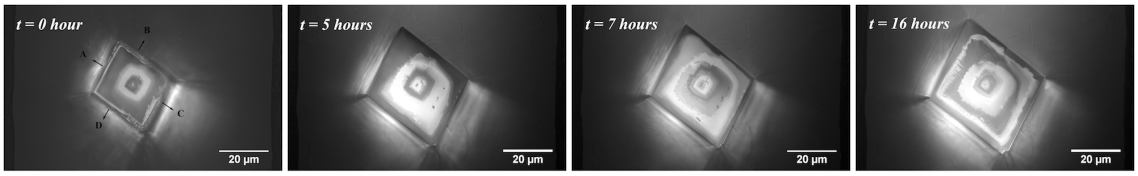

Figure 4. 16 hours growth of crystal D. The Ca^{2+} concentration here was 0.7 mM. **This one needs to be studied in a bit more detail. Is it smooth?**

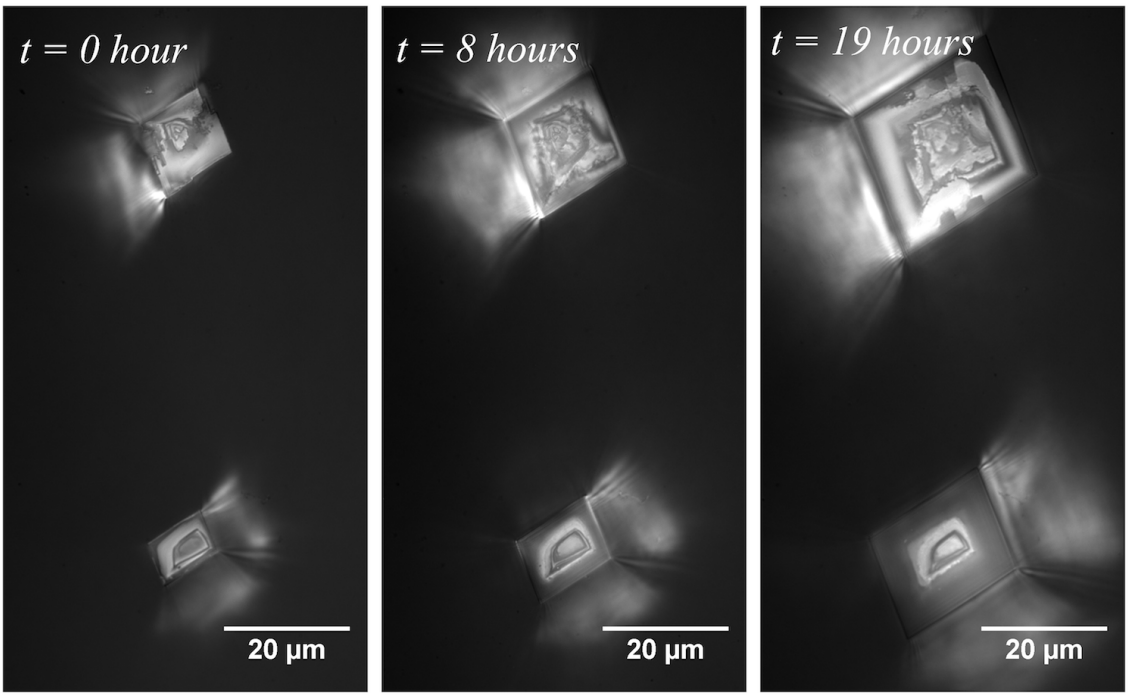

Figure 5. 19 hours growth of crystals E and F. The Ca^{2+} concentration here was 0.7 mM. This experiment shows the two classes of confined crystals contacts at the same time: intermittent (top) and smooth (bottom)

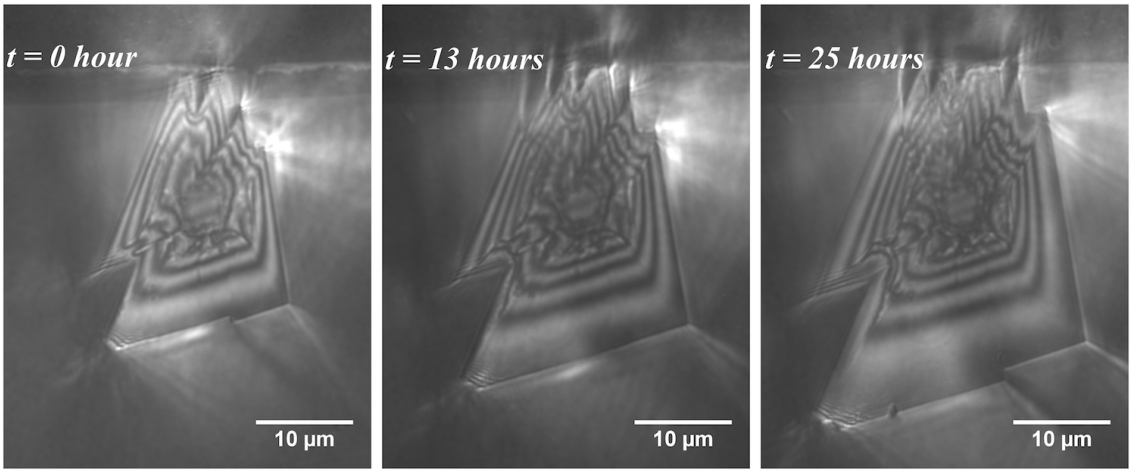

Figure 6. 25 hours growth of crystal G. The Ca^{2+} concentration here was 0.7 mM. Flow direction from left to right? The confined contact surface is not a 104 surface

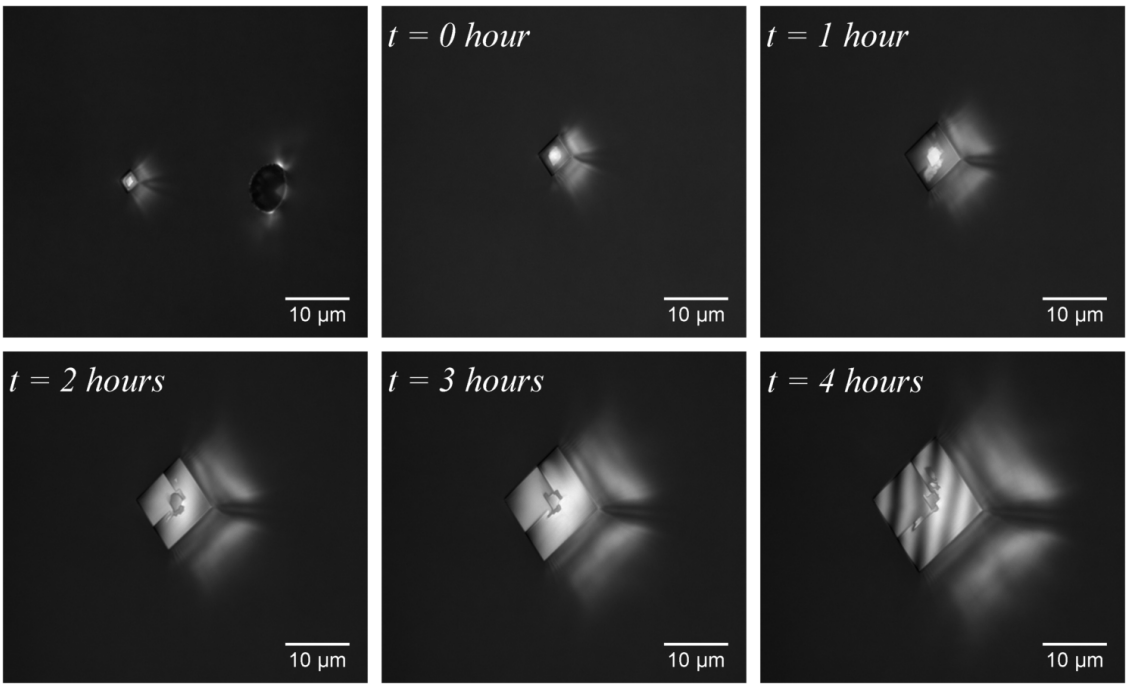

Figure 7. 4 hours growth of crystal H. The Ca^{2+} concentration here was 0.7 mM. The crystal seems initially smooth and flat. After 1 hour it develops a "defect" and continues to grow two separate flat surfaces at different heights and the crystal surface tilts with respect to the glass surface.

2.3. Summary of growth rates

Table 1. Summary of growth rates for all the crystals.

Name	**Concentration** c mM	**Upwards growth rate** dz/dt nm/h	**Smooth/ intermittent**	**outwards growth rate** dr/dt nm/h	**relative growth rate** $100 \cdot dz/dr$ %
A (crystal 12)	0.8	25→ 1.5	Smooth	310 ± 9	(8→)0.5
B (crystal 4)	0.7	180 ± 5	Intermittent	850 ± 10	21
C (crystal 11)	0.8	151→ 0	Smooth	1430 ± 70	11(→)0
D (crystal 5)	0.7	20 ± 1	smooth?	290 ± 30	7
E (crystal 17 top)	0.8	41 ± 1	Intermittent	250 ± 20	16
F (crystal 17 bottom)	0.8	8 ± 1→ 0	Smooth	190 ± 30	(4→)0
G (crystal 2)	??	20→ 4	Smooth, Not 104	130 ± 20	(15→)3
H (crystal 12, fringe11)	0.8	103 ± 6	Tilted	1240 ± 50	8

Table 1 summarizes the growth rates of all the crystals presented in this paper. One observes that there is a large variation in growth rates both vertically and outwards at nominally identical conditions. The ratio of the vertical to the outwards growth rates shows that the intermittent contact (or wobbling) and tilted crystals grow consistently at a higher rate than the smooth contacts. Smooth contacts also tend to slow down or stop growing upwards after a certain time.

Peer-reviewed version available at Crystals 2017, 7, 361; doi:10.3390/cryst7120361

3. Discussion and conclusions

3.1. Disjoining pressure - the hovering crystal

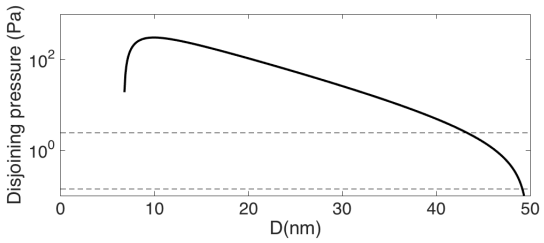

Figure 8. Disjoining pressure of silica on calcite surface in saturated $CaCO_3$ solution (whole drawn line). Minimum and maximum pressures on the contact area of the confined crystal surface with the glass are indicated with dashed lines.

In order to check whether this range of pressures (0.14-2.42 Pa) can be sustained by the disjoining pressure of a thick fluid film we have calculated disjoining pressures using the DLVO theory for silica-calcite. We have used equation (S4) from Diao and Espinosa-Marzal [13] and their parameters for a saturated $CaCO_3$ solution (0.51 mM Ca^{2+}) (Table S1 og S3 in [13]) and the Hamaker constant computed by their equation (S3). The resulting curve in Figure 8 shows that the disjoining pressure for silica - calcite probably more than is large enough to support the crystal at distances of 40 nm and more. The fact that the crystal seems to move approximately between 10-20 and 30-40 nm suggests that the disjoining pressure between silica and calcite is slightly larger than between our cover glass and calcite.

3.2. Rim edge jumps

We find two possible explanations for the jumps in inner rim edge and change in contact distance h:

1. Something lifts the crystal slowly off the glass surface making h increase linearly in time by about 20 nm until it collapses back to a smaller value. The rim width, w increases because h increases. If the rim width is limited by diffusion transport it should scale as $w^2 \propto h$. The present data is not sufficiently accurate to decide if the relation between rim width and height is linear or quadratic.
2. The anisotropic surface energy of the crystal causes the atomic layer growth at the nanoconfined rim to continue to lower concentrations. When the surface energy can no longer "draw" the inner edge inwards the inner edge position jumps to a position further out. As the area of contact increases the normal stress (due to the weight of the crystal) decreases and the disjoining pressure (which decreases with distance h) is balanced at a larger distance h.

The interpretation of Figure 1 **D** and Figure 8 together makes it plausible that the disjoining pressure is responsible for moving the crystal up and down depending on the area of contact. We therefore find the second explanation for the jump in inner rim edge more plausible.

3.3. Smooth and intermittent contacts

The much faster growth rate of Crystal B (see Figure 2) may be explained by larger distance h between most of the contact rim and the glass. The parts of the rim that are not in closest contact grow faster, tilting the crystal this way and that. The crystal "wobbles" its way up at a remarkably steady pace (see Figure 10).

We conclude that smooth contacts arrest upwards growth. Roughness or defects that spur intermittent contacts allow transport in the nanoconfined contact area and continued upwards growth.

Intermittent contacts look like ex situ contacts observed by Røyne and Dysthe [12] on NaClO3. The large variations in growth modes and arrest of upwards growth explains why the ex situ contact width measurements in that study did not fit with isotropic continuum theory.

This has implications for further experiments and modelling of the force of crystallization: Experiments with smooth contacts will yield no appreciable forces during timescales attainable in in situ lab experiments. Models of smooth contacts will not bring our understanding further, one needs to quantify and include effects of disorder.

4. Materials and Methods

The microfluidic network and flow control system to nucleate calcium carbonate crystals in a limited area that permits imaging access, to remove other polymorphs than calcite, to control stable saturation conditions at the growing crystal surface, permit slow growth of rhombohedral crystals from the nuclei, measure growth rates and avoid clogging of microfluidic device due to crystal growth elsewhere in the device has been described in detail in [14]. The main idea is sketched in Figure 9. $CaCl_2$ solution and Na_2CO_3 solution at equal concentration and flow rate are introduced in two inlets and in the third inlet distilled water is introduced to control the total concentration c of the $CaCO_3$ + NaCl solution in the main channel. The growth rate of the crystal (green in Figure 9) depends on the supersaturation c/c_0, where c_0 is the equilibrium concentration. There are many definitions of supersaturation, but in this dilute system we will use the simplest definition and consider linearized transport and growth laws close to the equilibrium concentration c_0 measured in situ as the concentration where the crystal neither grows nor dissolves, $c_0 = 0.50 \pm 0.02$ mM.

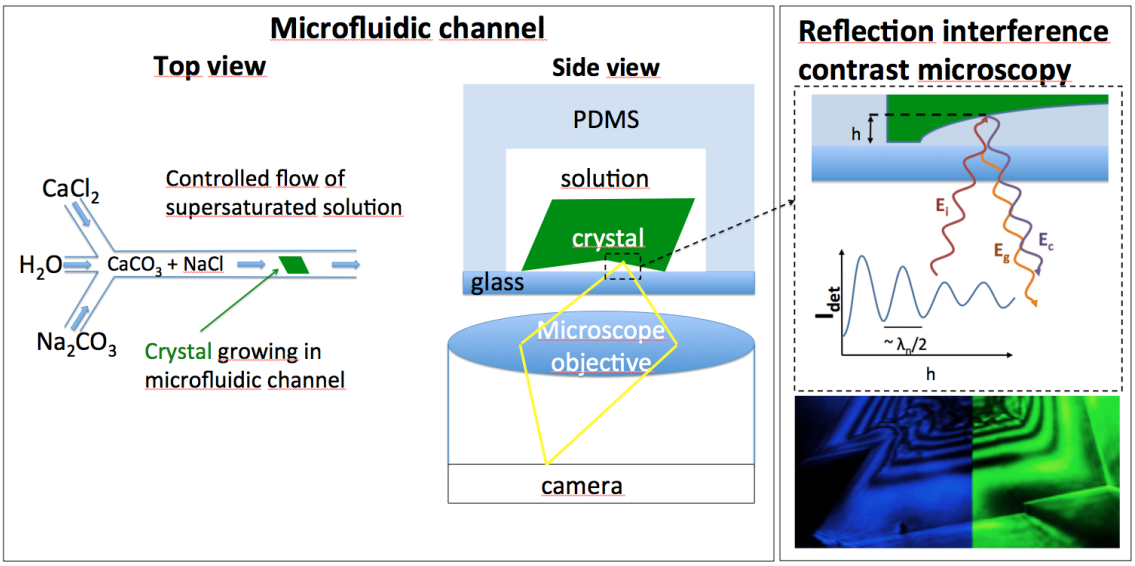

Figure 9. Controlled growth of calcite crystals in a microfluidic device studied by reflected interference microscopy (RICM). **Left:** Top view of microfluidic channel shows how fluids are introduced and mixed to ensure stable supersaturation at the crystal surfaces. The microfluidic device rests on an inverted microscope to allow high resolution imaging of the crystal in situ during growth.The crystal grows at all surfaces but the surface studied here is confined by the glass surface on which the crystal rests. **Right:** Principle of reflection interference contrast microscopy (RICM) that yields a measured intensity I variation with distance h between crystal and glass. The image shows a crystal imaged with blue and green light. The dark fringes are aligned only at the rim of the crystal and out of phase towards the middle of the surface. The phase shift is due to the difference in wavelength and a growing distance h between the crystal and glass towards the middle of the surface.

Preprints (www.preprints.org) | NOT PEER-REVIEWED | Posted: 8 August 2017 doi:10.20944/preprints201708.0028.v1

Peer-reviewed version available at Crystals 2017, 7, 361; doi:10.3390/cryst7120361

The crystal growth at the confined interface between crystal and glass is measured by reflection interference contrast microscopy (RICM). The basic principle of RICM is illustrated in Figure 9. The incident light from the microscope is reflected both from the crystal-water interface and from the glass-water interface. Thus, a part

$$I_r \propto E_g^2 + E_c^2 + E_g E_c \cos(4\pi h n/\lambda + \pi) \tag{1}$$

of the total intensity $I = I_0 + I_r$ reaching the detector is given by the interference of these two reflected parts of the incident light, where E_g is the electromagnetic wave amplitude reflected at the glass-water interface, E_c is the electromagnetic wave amplitude reflected at the crystal-water interface, λ is the wavelength of the light and h is the distance between the glass and n is the refractive index of water. I_0 denotes the part of the light reaching the detector by scattering at other interfaces of the system. Here, the light is represented by its central beam. Effects of the finite aperture of the imaging systems are not considered. As explained above, when the crystal reaches a certain size the crystal growth at the centre of the crystal stops because the transport of ions from solution is less than the consumption of ions by crystal growth. Therefore one can measure the growth rate $v = dh/dt$ of the crystal at the rim (the confined crystal-glass interface) by measuring the change of intensity $I(t)$ with time.

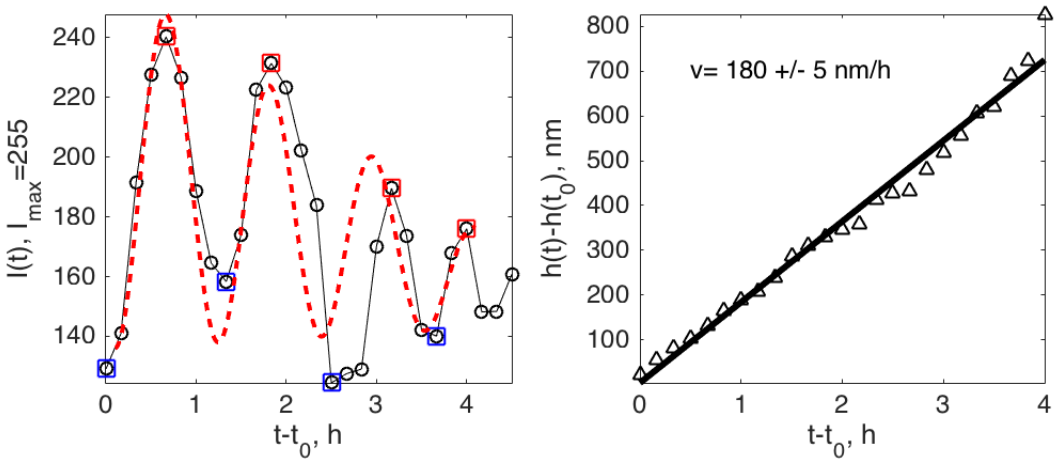

Figure 10. Left: Intensity in the middle of crystal B (see Figure 2) surface with time. Circles denote data from images, blue and red squares are data points used to rescale amplitude before applying arcsine. Red dashed line shows fit to data. **Right:** Triangles are height calculated from intensity data as function of time and black line is least squares fit.

Figure 10 shows intensity data $I(t)$ from the middle of crystal B (see Figure 2) surface with time. The minima (blue squares) and maxima (red squares) are used to rescale all intensity data points in between to the range [-1,1]: $\hat{I}(t)$. Then the distance h between crystal and glass is

$$h(t) - h(t_0) = \frac{\lambda}{4n}(2i + \pi \arcsin \hat{I}), \tag{2}$$

where i is an integer counting the number of periods. The right hand side of Figure 10 shows the $h(t) - h(t_0)$ calculated from the intensity data on the left. The least squares fit yields the growth rate v with standard deviation. This value of v is used with a smooth amplitude function to compare the fit (red dashed line) to the original data on the left side of Figure 10.

Supplementary Materials: The following are available online at www.mdpi.com/link, Video S1.avi.

Acknowledgments: This project has received funding from the European Union's Horizon 2020 research and innovation programme under the Marie Sklodowska-Curie grant agreement no. 642976 (ITN NanoHeal) and from the Norwegian Research Council grant no. 222386.

Author Contributions: L.L designed and performed experiments, analyzed data and contributed to writing the paper, D.K.D. conceived and designed the experiments, analyzed data and wrote the paper, A.R. and F.K. contributed to analysis of data and writing the paper.

Conflicts of Interest: The authors declare no conflict of interest.

Abbreviations

The following abbreviations are used in this manuscript:

MDPI: Multidisciplinary Digital Publishing Institute
RICM: Reflection interference contrast microscopy

References

1. Wilkinson, B.H. Biomineralization, paleoceanography, and the evolution of calcareous marine organisms. *Geology* **1979**, *7*, 524–527.
2. Stephens, C.J.; Ladden, S.F.; Meldrum, F.C.; Christenson, H.K. Amorphous Calcium Carbonate is Stabilized in Confinement. *Advanced Functional Materials* **2010**, *20*, 2108–2115.
3. Gratier, J.p.; Dysthe, D.K.; Renard, F. The role of pressure solution creep in the ductility of the Earth ' s upper crust. *Advances in Geophysics* **2013**, *54*, 1–112.
4. Flatt, R.J.; Caruso, F.; Sanchez, A.M.A.; Scherer, G.W. Chemo-mechanics of salt damage in stone. *Nature communications* **2014**, *5*, 4823.
5. Chang, C.F.; Chen, J.W. The experimental investigation of concrete carbonation depth. *Cement and Concrete Research* **2006**, *36*, 1760–1767.
6. Rothrock, E.P. On the force of crystallization of calcite. *Journal of Geology* **1925**, *33*, 80–83.
7. Gratier, J.P.; Frery, E.; Deschamps, P.; Røyne, A.; Renard, F.; Dysthe, D.; Ellouz-Zimmerman, N.; Hamelin, B. How travertine veins grow from top to bottom and lift the rocks above them: The effect of crystallization force. *Geology* **2012**, *40*, 1015–1018.
8. Israelachvili, J.N. *Intermolecular and surface forces*; Academic Press, 2011; p. 674.
9. Dysthe, D.K.; Renard, F.; Porcheron, F.; Rousseau, B. Fluid in mineral interfaces—molecular simulations of structure and diffusion. *Geophysical Research Letters* **2002**, *29*, 13–14.
10. Weyl, P.K. Pressure solution and the force of crystallization: a phenomenological theory. *Journal of Geophysical Research* **1959**, *64*, 2001–2025.
11. Becker, G.F.; Day, A.L. The linerar force of growing crystals. *Proc. Washingt. Acad. Sci.* **1905**, *7*, 283–288.
12. Røyne, A.; Dysthe, D.K. Rim formation on crystal faces growing in confinement. *Journal of Crystal Growth* **2012**, *346*, 89–100.
13. Diao, Y.; Espinosa-Marzal, R.M. Molecular insight into the nanoconfined calcite–solution interface. *Proceedings of the National Academy of Sciences* **2016**, *113*, 12047–12052.
14. Li, L.; Sanchez, J.R.; Kohler, F.; R{\o}yne, A.; Dysthe, D.K. Microfluidic control of nucleation and growth of calcite. *arXiv:cond-mat* **2017**.